

# ChemComm

Chemical Communications

Accepted Manuscript

This article can be cited before page numbers have been issued, to do this please use: Y. Wang, M. Jin, Z. Chen, X. Hu, L. Pu, Z. Pei and Y. Pei, *Chem. Commun.*, 2020, DOI: 10.1039/D0CC04149A.



This is an Accepted Manuscript, which has been through the Royal Society of Chemistry peer review process and has been accepted for publication.

Accepted Manuscripts are published online shortly after acceptance, before technical editing, formatting and proof reading. Using this free service, authors can make their results available to the community, in citable form, before we publish the edited article. We will replace this Accepted Manuscript with the edited and formatted Advance Article as soon as it is available.

You can find more information about Accepted Manuscripts in the [Information for Authors](#).

Please note that technical editing may introduce minor changes to the text and/or graphics, which may alter content. The journal's standard [Terms & Conditions](#) and the [Ethical guidelines](#) still apply. In no event shall the Royal Society of Chemistry be held responsible for any errors or omissions in this Accepted Manuscript or any consequences arising from the use of any information it contains.

## COMMUNICATION

## Tumor Microenvironment Responsive Supramolecular Glyco-Nanovesicles Based on Diselenium-Bridged Pillar[5]arene Dimer for Targeting Chemotherapy

Yang Wang, Ming Jin, Zelong Chen, Xianjun Hu, Liang Pu, Zhichao Pei and Yuxin Pei\*

Received 00th January 20xx,  
Accepted 00th January 20xx

DOI: 10.1039/x0xx00000x

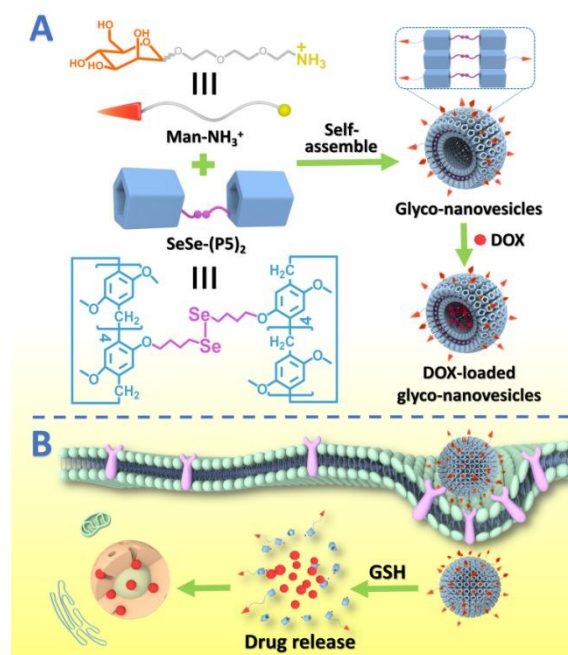
**Supramolecular glyco-nanovesicles (SeSe-(P5)<sub>2</sub>⊃Man-NH<sub>3</sub><sup>+</sup>) based on the host-guest complex of diselenium-bridged pillar[5]arene dimer and mannose derivative have been successfully developed for the first time, which possessed tumor microenvironment-responsiveness and specific targetability due to their diselenium bonds and mannose units, respectively.**

Nowadays, in spite of chemotherapy is one of the most effective treatments for cancer, its clinical application is limited, resulting from the lack ability of specific targeting or on-demand drug release.<sup>1,2</sup> During the past decades, smart supramolecular drug delivery systems (SDDS), possessing the stimuli-responsiveness and targetability, have been developed, based on dynamic self-assembly process with noncovalent bonds, especially the host-guest interactions.<sup>3-7</sup> Furthermore, the tumor microenvironment (TME) is a complex integrated system, which features high glutathione (GSH) level, low pH, and overproduced hydrogen peroxide. Therefore, TME could supply intracellular stimuli for SDDS to realize targeting therapy.<sup>8,9</sup>

Supramolecular nanovesicles are widely used as nanocarriers to encapsulate drugs resulted from their unique cavities. They are obtained by amphiphilic host-guest complexes with multifunctional units through dynamic self-assembly, causing the susceptibility to exogenous or endogenous stimuli accompanied by changes in morphology.<sup>10,11</sup> Carbohydrates, as attractive hydrophilic biomolecules with good biocompatibility and specific recognition of glycoproteins, are gaining more interests in construction of supramolecular glyco-nanovesicles.<sup>12-15</sup> Thus, supramolecular glyco-nanovesicles composed of carbohydrate derivatives and macrocyclic host molecules have potential in targeting chemotherapy.<sup>16,17</sup>

Pillar[n]arenes, as an emerging category of macrocyclic molecules, composed of hydroquinone units which are connected by methylene bridges at the para-position.<sup>18,19</sup>

Attributed to the versatile chemical modifiability and unique symmetrical structures,<sup>20-23</sup> pillar[n]arenes have been increasingly popular host molecules in supramolecular chemistry over decade and utilized in the multifunctional SDDS in recent years.<sup>24-31</sup> Most application of pillar[n]arenes is based on monomeric pillar[n]arenes. Until now, another intriguing category of pillar[n]arenes, bridged pillar[n]arene dimer, are less reported and rarely investigated in drug delivery systems.<sup>32-34</sup> For instance, Wang *et al.* reported paclitaxel-loaded nanoparticles based on disulphide-bridged pillar[5]arene dimer using a microemulsion method without the involvement of any amphiphilic structures.<sup>34</sup> Compared with sulfur, selenium has



**Scheme 1** Illustration of (A) the construction of supramolecular glyco-nanovesicles (SeSe-(P5)<sub>2</sub>⊃Man-NH<sub>3</sub><sup>+</sup>) and (B) their TME-responsive targeting chemotherapy.

Shaanxi Key Laboratory of Natural Products & Chemical Biology,  
College of Chemistry & Pharmacy, Northwest A&F University, Yangling 712100,  
P. R. China. E-mail: peiyx@nwfau.edu.cn; Fax: +86-29-8709-1196;  
Electronic Supplementary Information (ESI) available: See DOI: 10.1039/x0xx00000x

lower electronegativity and a large atomic radius, resulting in the lower bond energy of diselenium bonds (172 kJ/mol) than disulfide bonds (240 kJ/mol).<sup>35–37</sup> Hence, we supposed that the drug delivery systems containing diselenium bonds should have more ideal drug release behavior than disulfide bonds upon TME. And to the best of our knowledge, there is no report of multifunctional SDDS based on diselenium-bridged pillar[5]arene dimer for targeting chemotherapy.

In this work, we reported a supramolecular glyco-nanovesicle (SeSe-(P5)<sub>2</sub>⊃Man-NH<sub>3</sub><sup>+</sup>) with TME-responsiveness based on the host-guest complex of diselenide-containing pillar[5]arene dimer (SeSe-(P5)<sub>2</sub>) and mannose derivative (Man-NH<sub>3</sub><sup>+</sup>) for targeting chemotherapy, where the targetability derives from the mannose residue of Man-NH<sub>3</sub><sup>+</sup>, meanwhile TME-responsiveness derives from the diselenium bonds of SeSe-(P5)<sub>2</sub> (Scheme 1). Thereby, the drug-loaded supramolecular glyco-nanovesicles could not only effectively target to cancer cells, but also implement TME-responsiveness to on-demand drug release.

Firstly, SeSe-(P5)<sub>2</sub> and Man-NH<sub>3</sub><sup>+</sup> were synthesized by following previously reported methods,<sup>38</sup> and characterized by <sup>1</sup>H NMR (Fig. S1–S7, ESI<sup>†</sup>).

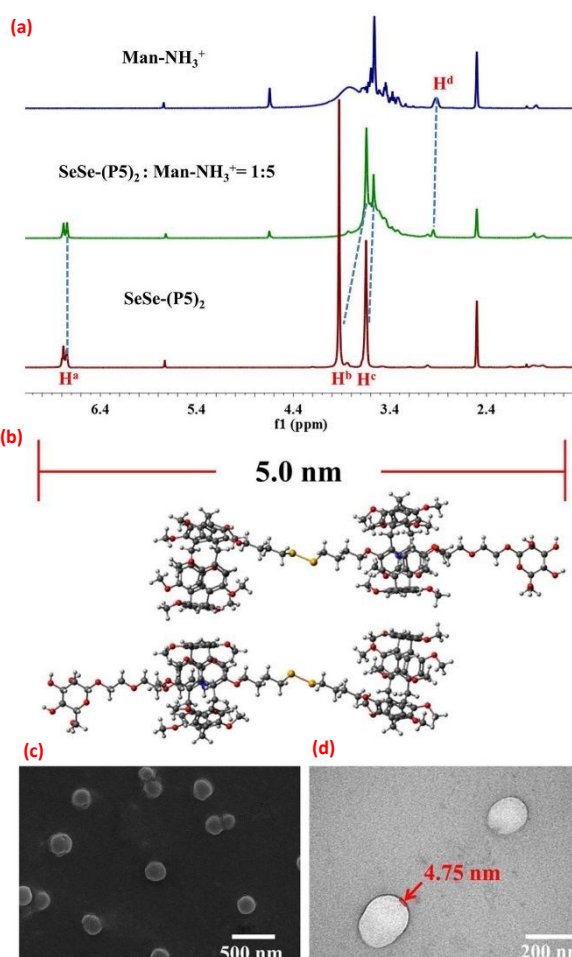


**Fig. 1** (a) <sup>1</sup>H NMR spectra (500 MHz, DMSO-*d*<sub>6</sub>, 298 K): (top) Man-NH<sub>3</sub><sup>+</sup> (25 mM); (middle) SeSe-(P5)<sub>2</sub> : Man-NH<sub>3</sub><sup>+</sup> = 1 : 5; (bottom) SeSe-(P5)<sub>2</sub> (5 mM); (b) The energy-minimized structure of SeSe-(P5)<sub>2</sub>⊃Man-NH<sub>3</sub><sup>+</sup> (ball and stick mode); (c) SEM image and (d) TEM image of SeSe-(P5)<sub>2</sub>⊃Man-NH<sub>3</sub><sup>+</sup> glyco-nanovesicles.

We mixed Man-NH<sub>2</sub> and SeSe-(P5)<sub>2</sub> in 800 μL DMSO-*d*<sub>6</sub> with 4 μL deuterium-hydrochloric acid via <sup>1</sup>H NMR to verify if there presented host-guest interactions between them. As shown in Fig. 1a, it revealed the obvious upfield chemical shifts of phenyl protons (H<sup>a</sup>), methylene protons (H<sup>b</sup>) and slight upfield chemical shifts of methoxy protons (H<sup>c</sup>) of SeSe-(P5)<sub>2</sub>. Meanwhile, the methylene protons (H<sup>d</sup>) adjacent to the ammonium ion of Man-NH<sub>3</sub><sup>+</sup> presented slight downfield chemical shifts, which indicated the formation of host-guest complex (H<sup>a-d</sup> defined in Fig S3 and S7, ESI<sup>†</sup>).<sup>39</sup> Unlike what we expected that one mole of SeSe-(P5)<sub>2</sub> would combine with two moles of Man-NH<sub>3</sub><sup>+</sup>, the stoichiometry of the SeSe-(P5)<sub>2</sub>⊃Man-NH<sub>3</sub><sup>+</sup> complexation via Job's plot method (Fig. S8, S9, ESI<sup>†</sup>) showed that the 1 : 1 binding stoichiometry between SeSe-(P5)<sub>2</sub> and Man-NH<sub>3</sub><sup>+</sup>. We supposed that the possible assembled state should present as Fig. 1b.

To construct SeSe-(P5)<sub>2</sub>⊃Man-NH<sub>3</sub><sup>+</sup> glyco-nanovesicles based on the complexation between SeSe-(P5)<sub>2</sub> and Man-NH<sub>3</sub><sup>+</sup>, a mixed solution of SeSe-(P5)<sub>2</sub> and Man-NH<sub>3</sub><sup>+</sup> in H<sub>2</sub>O/THF (10 : 1 in v/v) was sonicated for 1 h and then stood overnight. SEM and TEM images (Fig. 1c, and d, respectively) indicated the formation of a vesicular structure with hollow spherical morphology and the film with a thickness of 4.75 nm, which was matched with the theoretical calculation value (Fig. 1b). The dynamic light scattering (DLS) analysis (Fig. S10a, ESI<sup>†</sup>) showed that the glyco-nanovesicles have an average size of 270 nm. Furthermore, the critical aggregation concentration (CAC) of SeSe-(P5)<sub>2</sub>⊃Man-NH<sub>3</sub><sup>+</sup> was quantitatively found to be 10.4 μg/mL through the water surface tension method (Fig. S11, ESI<sup>†</sup>).

Upon the methyl thiazole tetrazolium (MTT) assay, the cytotoxicity of glyco-nanovesicles was evaluated. HepG2 human hepatoma cells, MCF-7 breast cancer cells, and 293T healthy human kidney cells were incubated with SeSe-(P5)<sub>2</sub>⊃Man-NH<sub>3</sub><sup>+</sup> glyco-nanovesicles at various concentrations for different time periods. The relative cell viabilities (Fig. S12, ESI<sup>†</sup>) showed that even if at high concentration (200 μg/mL) of SeSe-(P5)<sub>2</sub>⊃Man-NH<sub>3</sub><sup>+</sup> glyco-nanovesicles the relative cell viabilities were still at high levels,

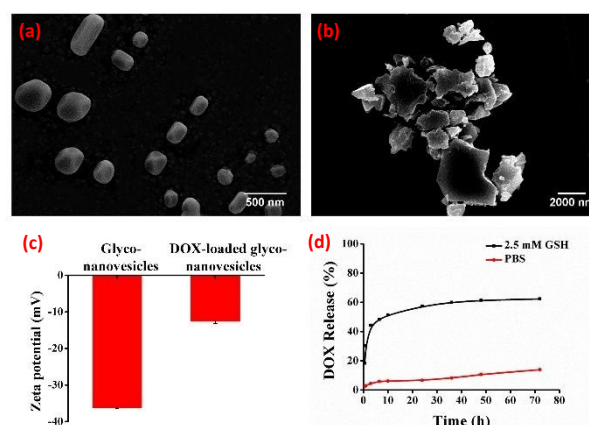


**Fig. 2** (a) SEM images of DOX-loaded SeSe-(P5)<sub>2</sub>⊃Man-NH<sub>3</sub><sup>+</sup> glyco-nanovesicles (scale bar: 500 nm); (b) SEM images of DOX-loaded SeSe-(P5)<sub>2</sub>⊃Man-NH<sub>3</sub><sup>+</sup> glyco-nanovesicles in the presence of 10 mM GSH (scale bar: 2000 nm); (c) Zeta potential of SeSe-(P5)<sub>2</sub>⊃Man-NH<sub>3</sub><sup>+</sup> glyco-nanovesicles with or without DOX-loaded; (d) DOX release profile of the DOX-loaded SeSe-(P5)<sub>2</sub>⊃Man-NH<sub>3</sub><sup>+</sup> glyco-nanovesicles in 2.5 mM GSH and PBS, respectively.

which revealed the good biocompatibility of the supramolecular glyco-nanovesicles.

Then, the drug encapsulation efficiency, and stimuli-responsive release behavior of glyco-nanovesicles were investigated using doxorubicin hydrochloride (DOX) as a model anticancer drug. Upon encapsulating DOX into the cavity of the SeSe-(P5)<sub>2</sub>Man-NH<sub>3</sub><sup>+</sup> glyco-nanovesicles (the preparation details were shown in ESI<sup>†</sup>), SEM (Fig. 2a) showed that the morphology of DOX-loaded SeSe-(P5)<sub>2</sub>Man-NH<sub>3</sub><sup>+</sup> glyco-nanovesicles changed to irregular nanoparticles. The change of the morphology may result from the electrostatic and  $\pi$ - $\pi$  stacking interactions between DOX and the complex of SeSe-(P5)<sub>2</sub>Man-NH<sub>3</sub><sup>+</sup>. Furthermore, the DOX-loaded glyco-nanovesicles had different morphology compared to the spherical vesicles formed by pristine DOX (Fig. S13, ESI<sup>†</sup>).

And the DLS results (Fig. S10b, ESI<sup>†</sup>) showed the average size of DOX-loaded glyco-nanovesicles increased to 319 nm. In addition, the zeta potential measurements (Fig. 2c) and UV-Vis spectrum (Fig. S14, ESI<sup>†</sup>) indicated that DOX was successfully encapsulated ( $\zeta$ -potential = -12.6 mV). Furthermore, the drug loading efficiency and loading content of the glyco-nanovesicles were determined to be 69.1% and 21.3%, respectively.

To investigate the release behavior of DOX from SeSe-(P5)<sub>2</sub>Man-NH<sub>3</sub><sup>+</sup> glyco-nanovesicles, the change of morphology and the amount of released DOX were monitored upon neutral environment with GSH. As shown in Fig. 2b, the SEM image of the SeSe-(P5)<sub>2</sub>Man-NH<sub>3</sub><sup>+</sup> glyco-nanovesicles showed that the morphology of the glyco-nanovesicles was intensely changed and clustered into large pieces after incubated with GSH (10 mM). The DOX release profiles (Fig. 2d) revealed that DOX was inappreciably released with the cumulative release amount of 13% under neutral conditions within 72 h. While high cumulative release amount of 62% within 72 h was obtained upon the neutral environment with 2.5 mM GSH. The results demonstrated that the DOX-loaded glyco-nanovesicles had good stability without obvious premature leakage and exhibited responsiveness to GSH. Compared with the 17% drug release of paclitaxel-loaded nanoparticles based on disulphide-bridged pillar[5]arene dimer upon 10 mM GSH for 86 h, which was reported by Wang *et al.*, SeSe-(P5)<sub>2</sub>Man-NH<sub>3</sub><sup>+</sup> glyco-nanovesicles showed superior drug release efficiency. Moreover, the DOX-loaded glyco-nanovesicles were incubated with HepG2 cells for 2, 4, 12 h, respectively, and the intracellular DOX fluorescence intensity was observed with a confocal laser scanning microscope (CLSM) to investigate the cellular uptake of glyco-nanovesicles. The CLSM images (Fig. 3a) showed the fluorescence intensity of DOX (red channel) was increased with the prolongation of incubated time, meanwhile, the fluorescence of DOX had a good overlap with the fluorescence of the nuclei (blue channel). The results of semi-quantitative analysis (Fig. 3b) were matched with the fluorescence images. This result demonstrated that DOX-loaded glyco-nanovesicles could be effectively uptake by HepG2 cells, and released DOX to enter the nuclei. To evaluate the targetability of the glyco-nanovesicles, HepG2 cells and 293T cells were incubated with DOX-loaded glyco-nanovesicles for 4 h. As expected, the red fluorescence of DOX in 293T cells (Fig. S15, ESI<sup>†</sup>) was much weaker, compared with that in HepG2 cells. On the other hand, the CLSM images (Fig. 3c) showed that the fluorescence intensity of DOX was significant decreased when the HepG2 cells were pre-incubated with mannose for 4 h. It means that the cellular uptake of HepG2 cells mediated by mannose to mannose receptors was reduced due

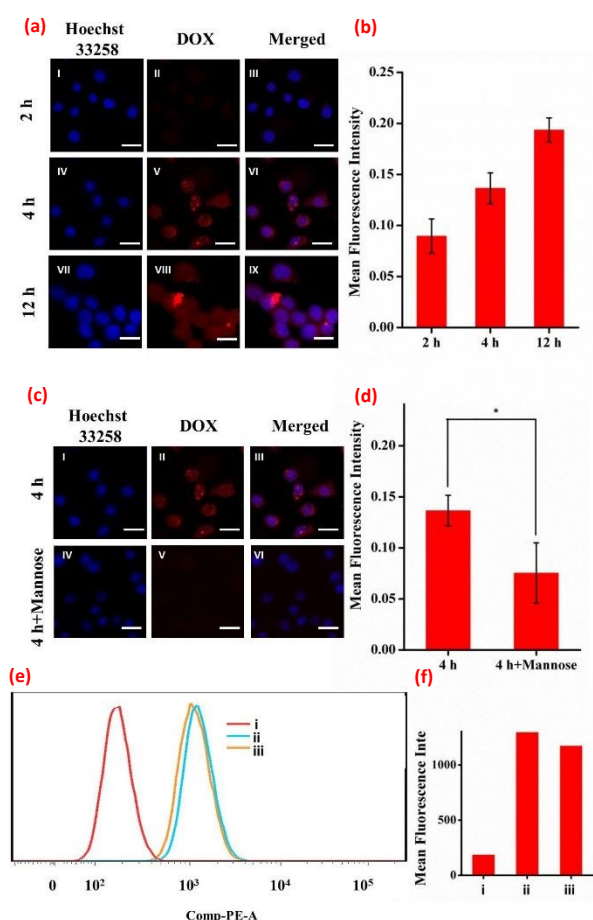


**Fig. 3** (a) CLSM images of HepG2 cells incubated with DOX-loaded SeSe-(P5)<sub>2</sub>Man-NH<sub>3</sub><sup>+</sup> glyco-nanovesicles for 2, 4, 12 h, respectively (DOX concentration: 5  $\mu$ M, scale bar: 20  $\mu$ m); (b) Mean fluorescence intensity of DOX in HepG2 cells (n = 50); (c) CLSM images of HepG2 cells incubated with DOX-loaded SeSe-(P5)<sub>2</sub>Man-NH<sub>3</sub><sup>+</sup> glyco-nanovesicles upon different treatments (with or without pre-incubation of mannose for 4 h, DOX concentration: 5  $\mu$ M, scale bar: 20  $\mu$ m); (d) Mean fluorescence intensity of DOX in HepG2 cells with different treatments \*p < 0.05 (n = 50); (e) Flow cytometry analysis and (f) mean fluorescence intensity of DOX in HepG2 cells with different treatments. i: PBS, ii: DOX-loaded glyco-nanovesicles, iii: DOX-loaded glyco-nanovesicles + Mannose (DOX concentration: 5  $\mu$ M).

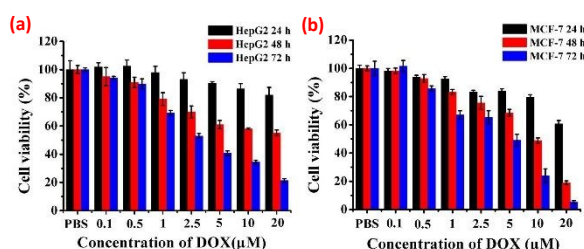


**Fig. 4** Cell viability of (a) HepG2 cells and (b) MCF-7 cells incubated with DOX-loaded SeSe-(P5)<sub>2</sub>Man-NH<sub>3</sub><sup>+</sup> glyco-nanovesicles at different DOX concentrations for 24, 48 and 72 h (n = 6).

to the blocked mannose receptors. The same conclusion could be drawn from flow cytometry analysis of HepG2 cells (Fig. 3e, f) and MCF-7 cells (Fig. S16, ESI<sup>†</sup>) after incubation with PBS, DOX-loaded glyco-nanovesicles (with or without pre-incubation of mannose for 4 h), respectively.

The anticancer efficiency *in vitro* of DOX-loaded glyco-nanovesicles was further investigated via MTT assay. The HepG2 and MCF-7 cells were separately incubated with DOX-loaded glyco-nanovesicles for different time periods. As shown in Fig. 4, the cell viabilities of HepG2 and MCF-7 cells were obviously decreased with the prolongation of incubating time and the increasement of DOX concentration. Under the same conditions, the cell viability of 293T cells was higher than the cell viabilities of HepG2 cells and MCF-7 cells, which was likely due to the lower concentration of GSH and lower expression of mannose receptor in normal cells (Fig. S17, ESI<sup>†</sup>). Furthermore, the glyco-nanovesicles effectively reduced the toxicity of free DOX to 293T cells, although its cytotoxicity to cancer cells was not as good as that of free DOX owing to the slow release of DOX from the loaded-vesicles (Fig. S18, ESI<sup>†</sup>). The results demonstrated that the glyco-nanovesicles not only had a good killing effect on cancer cells, but also could reduce the toxicity of drugs to normal cells.

In summary, we have successfully designed and fabricated supramolecular glyco-nanovesicles based on pillar[5]arene dimer via the host-guest interactions between SeSe-(P5)<sub>2</sub> and Man-NH<sub>3</sub><sup>+</sup>. The glyco-nanovesicles possessed TME-responsiveness and targetability of cancer cell, owing to the diselenium bonds and mannose residue, respectively. Besides, it had good biocompatibility and could effectively accumulate in cancer cells to release DOX via the cleavage of diselenium bonds to achieve selective cytotoxicity. Therefore, this work provides a progressive example for SDDS based on pillar[n]arenes, which has enriched the application of pillar[n]arene dimer in the fields of biomaterials and biological medicine.

## Conflicts of interest

There are no conflicts to declare.

## Acknowledgements

This research work was supported by the National Natural Science Foundation of China (21772157 and 21877088).

## Notes and references

- J. Zhou, G. Yu and F. Huang, *Chem. Soc. Rev.*, 2017, **46**, 7021-7053.
- S. Tinkov, G. Winter, C. Coester and R. Bekerredjian, *Journal of Controlled Release*, 2010, **143**, 143-150.
- M. J. Webber and R. Langer, *Chem. Soc. Rev.*, 2017, **46**, 6600-6620.
- Q. Duan, Y. Cao, Y. Li, X. Hu, T. Xiao, C. Lin, Y. Pan and L. Wang, *J. Am. Chem. Soc.*, 2013, **135**, 10542-10549.
- M. X. Wu, J. Gao, F. Wang, N. Song, X. Jin, P. Mi, J. Tian, J. Luo, F. Liang and Y. W. Yang, *Small*, 2018, **14**, 1704440.
- Y. Cao, X. Y. Hu, Y. Li, X. Zou, S. Xiong, C. Lin, Y. Z. Shen and L. Wang, *J. Am. Chem. Soc.*, 2014, **136**, 10762-10769.
- Y. Chang, K. Yang, P. Wei, S. Huang, Y. Pei, W. Zhao and Z. Pei, *Angew. Chem. Int. Ed.*, 2014, **53**, 13126-13130.
- M. Zhang, X. Guo, M. Wang and K. Liu, *Journal of Controlled Release*, 2020, **323**, 203-224. DOI: 10.1039/D0CC04149A
- Y. Zhang, O. Eltayeb, Y. Meng, G. Zhang, Y. Zhang, S. Shuang and C. Dong, *New J. Chem.*, 2020, **46**, 2578-2586.
- X. D. Xu, L. Zhao, Q. Qu, J. G. Wang, H. Shi and Y. Zhao, *ACS Appl. Mater. Interfaces*, 2015, **7**, 17371-17380.
- X. Wu, Y. Li, C. Lin, X. Y. Hu and L. Wang, *Chem. Commun.*, 2015, **51**, 6832-6835.
- S. Cao, Z. Pei, Y. Xu and Y. Pei, *Chem. Mater.*, 2016, **28**, 4501-4506.
- D. Pati, S. Das, N. G. Patil, N. Parekh, D. H. Anjum, V. Dhaware, A. V. Ambade and S. Sen Gupta, *Biomacromolecules*, 2016, **17**, 466-475.
- L. Yin, Y. Chen, Z. Zhang, Q. Yin, N. Zheng and J. Cheng, *Macromol. Rapid Commun.*, 2015, **36**, 483-489.
- M. Gary-Bobo, Y. Mir, C. Rouxel, D. Brevet, I. Basile, M. Maynadier, O. Vaillant, O. Mongin, M. Blanchard-Desce, A. Morere, M. Garcia, J. O. Durand and L. Raehm, *Angew. Chem.*, 2011, **123**, 11627-11631.
- K. Yang, Y. Chang, J. Wen, Y. Lu, Y. Pei, S. Cao, F. Wang and Z. Pei, *Chem. Mater.*, 2016, **28**, 1990-1993.
- Y. Chang, C. Hou, J. Ren, X. Xin, Y. Pei, Y. Lu, S. Cao and Z. Pei, *Chem. Commun.*, 2016, **52**, 9578-9581.
- K. Yang, Y. Pei, J. Wen and Z. Pei, *Chem. Commun.*, 2016, **52**, 9316-9326.
- W. Feng, M. Jin, K. Yang, Y. Pei and Z. Pei, *Chem. Commun.*, 2018, **54**, 13626-13640.
- C. Li, *Chem. Commun.*, 2014, **50**, 12420-12433.
- T. Xiao, L. Zhou, L. Xu, W. Zhong, W. Zhao, X. Q. Sun and R. B. P. Elmes, *Chin. Chem. Lett.*, 2019, **30**, 271-276.
- Y. Han, C. Y. Nie, S. Jiang, J. Sun and C. G. Yan, *Chin. Chem. Lett.*, 2020, **31**, 275-278.
- J. Chen, H. Ni, Z. Meng, J. Wang, Y. Dong, C. Sun, Y. Zhang, L. Cui, J. Li, X. Jia, Q. Meng and C. Li, *Nat. Commun.*, 2019, **10**, 3546.
- Y. Cao, Y. Li, X. Y. Hu, X. Zou, S. Xiong, C. Lin and L. Wang, *Chem. Mater.*, 2015, **27**, 1110-1119.
- H. Zhu, H. Wang, B. Shi, L. Shangguan, W. Tong, G. Yu, Z. Mao and F. Huang, *Nat. Commun.*, 2019, **10**, 2412.
- Y. Wang, G. Ping and C. Li, *Chem. Commun.*, 2016, **52**, 9858-9872.
- G. Yu, W. Yu, L. Shao, Z. Zhang, X. Chi, Z. Mao, C. Gao and F. Huang, *Adv. Funct. Mater.*, 2016, **26**, 8999-9008.
- N. Song, X. Y. Lou, L. Ma, H. Gao and Y. W. Yang, *Theranostics*, 2019, **9**, 3075-3093.
- G. Yu and X. Chen, *Theranostics*, 2019, **9**, 3041-3074.
- H. Zhu, L. Shangguan, B. Shi, G. Yu and F. Huang, *Mater. Chem. Front.*, 2018, **2**, 2152-2174.
- Q. Hao, Y. Chen, Z. Huang, J. F. Xu, Z. Sun and X. Zhang, *ACS Appl. Mater. Interfaces*, 2018, **10**, 5365-5372.
- Y. Zhou, K. Jie, B. Shi and Y. Yao, *Chem. Commun.*, 2015, **51**, 11112-11114.
- C. L. Sun, H. Q. Peng, L. Y. Niu, Y. Z. Chen, L. Z. Wu, C. H. Tung and Q. Z. Yang, *Chem. Commun.*, 2018, **54**, 1117-1120.
- Q. Cheng, K. X. Teng, Y. F. Ding, L. Yue, Q. Z. Yang and R. Wang, *Chem. Commun.*, 2019, **55**, 2340-2343.
- G. Ma, J. Liu, J. He, M. Zhang and P. Ni, *ACS Biomater. Sci. Eng.*, 2018, **4**, 2443-2452.
- S. Ji, W. Cao, Y. Yu and H. Xu, *Angew. Chem. Int. Ed.*, 2014, **53**, 6781-6785.
- J. Xia, T. Li, C. Lu and H. Xu, *Macromolecules*, 2018, **51**, 7435-7455.
- Y. Wang, M. Z. Lv, N. Song, Z. J. Liu, C. Wang and Y. W. Yang, *Macromolecules*, 2017, **50**, 5759-5766.
- T. B. Wei, J. F. Chen, X. B. Cheng, H. Li, B. B. Han, H. Yao, Y. M. Zhang and Q. Lin, *Polym. Chem.*, 2017, **8**, 2005-2009.